Lab on a Chip

Cite this: *Lab Chip*, 2012, **12**, 1619

www.rsc.org/loc

PAPER

Acoustically enriching, large-depth aquatic sampler

Jonas Jonsson,* Sam Ogden, Linda Johansson, Klas Hjort and Greger Thornell

Received 5th January 2012, Accepted 13th February 2012
DOI: 10.1039/c2lc00025c

In marine biology, it is useful to collect water samples when exploring the distribution and diversity of microbial communities in underwater environments. In order to provide, *e.g.*, a miniaturized submersible explorer with the capability of collecting microorganisms, a compact sample enrichment system has been developed. The sampler is 30 mm long, 15 mm wide, and just a few millimetres thick. Integrated in a multilayer steel, polyimide and glass construction is a microfluidic channel with piezoelectric transducers, where microorganism and particle samples are collected and enriched, using acoustic radiation forces for gentle and labelless trapping. High-pressure, latchable valves, using paraffin as the actuation material, at each end of the microfluidic channel keep the collected sample pristine. A funnel structure raised above the surface of the device directs water into the microfluidic channel as the vehicle propels itself or when there is a flow across its hull. The valves proved leak proof to a pressure of 2.1 MPa for 19 hours and momentary pressures of 12.5 MPa, corresponding to an ocean depth of more than 1200 metres. By reactivating the latching mechanism, small leakages through the valves could be remedied, which could thus increase the leak-less operational time. Fluorescent particles, 1.9 μm in diameter, were successfully trapped in the microfluidic channel at flow rates up to 15 μl min^{-1}, corresponding to an 18.5 cm s^{-1} external flow rate of the sampler. In addition, liquid-suspended GFP-marked yeast cells were successfully trapped.

Introduction

Earth's oceans cover more than 70% of the planet's surface and have an average depth of 3800 metres. Life in this vast space is dominated by microorganisms, which have been found to inhabit all marine ecosystems investigated.[1] Prokaryotic microorganisms, including the archaea and bacteria domains, are generally found in the size range of 1–10 μm, while eukaryotes can be larger than this.[2]

Collection of water samples is essential in marine biology for exploration and classification of underwater environments, particularly when investigating the distribution and diversity of microbial communities. Commonly used collection devices include Nansen and Niskin bottles,[3] which are usually combined with conductivity, temperature and depth (CTD) sensors. Additionally, underwater vehicles can be fitted with water sampling devices.[4–6] In contrast to their ability to sample the open ocean, these samplers cannot be used in highly size-restricted environments, such as underneath ice shelves and in subglacial lakes, which must be accessed through long and narrow boreholes.

Sampling of subglacial lake waters for microorganisms has been performed,[7] using rather large devices directly underneath the boreholes. Since these environments are generally oligotrophic and sparsely populated, collection of sufficient pristine volumes presents a challenge. Sample enriching and concentration techniques, such as pumping water through a series of filters, can be employed to provide enough sample material for microbial analysis techniques.[6] However, mechanical filter systems tend to be cumbersome and the filtering of microorganisms generally requires a powerful and large pump to force water through the system.

The miniaturized submersible explorer *Deeper Access, Deeper Understanding* (DADU),[8] currently under development with such applications as to explore subglacial lakes or small cave systems, is only 20 cm long and 5 cm in diameter, and is thus easily transportable and deployable by hand, Fig. 1.

Due to the dimensions of the vehicle, about the size of two soda cans stuck together end-to-end, the use of miniaturization technologies for its subsystems and instrumentations is crucial to enable high functionality.[8]

The design goal of the DADU submersible is for it to be able to operate at depths down to 1000 metres. In order to provide the vehicle with the capability of collecting water and microorganism samples, a compact sample enrichment system has been developed. This sampler will be mounted in an instrument bay on the hull of the vehicle. The intention is to gently and labellessly trap microorganisms in a microfluidic channel using an acoustic standing wave field generated by miniaturized integrated transducers (MITs).[9] After a tailored collection time, during which

Ångström Space Technology Centre, Ångström Laboratory, Uppsala University, PO Box 534, Uppsala, Sweden. E-mail: jonas.jonsson@angstrom.uu.se; Fax: +46-(0)18-4713572; Tel: +46-(0)18-4717235

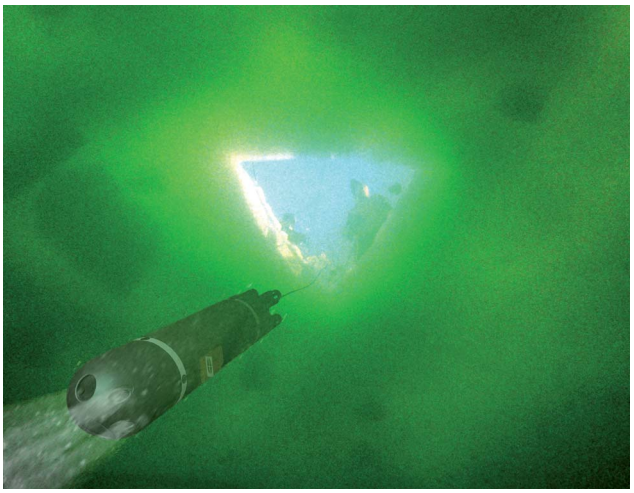

Fig. 1 Artistic visualization of the DADU submersible, facing to the lower left and carrying a sampler device, slightly brownish, on the right side of the hull, as it has been deployed into an ice-covered body of water.

either the submersible, through its movement, or ambient currents around a more or less stationary vehicle, force water through the device, the enriched sample will be sealed off by high-pressure, latchable valves,[10] before returning to the surface. Even during an extended mission, the samples will be kept pristine in the microfluidic channel by the valves, which only require power when changing their state, until examined in a full-scale laboratory facility.

This paper describes the design, manufacturing and characterization of this sampling device, using acoustic standing waves to trap and enrich a type of particle (polystyrene beads) and a type of microorganism (yeast) in the flow through the microfluidic channel, and high-pressure valves to ensure sealing of the microfluidic channel for transport to the surface.

Background

Acoustic waves can be generated by transducers made from a piezoelectric material, PZT, which changes its shape when stimulated electrically. By this, the transducer can be vibrated and made to transmit pressure waves into a medium, such as water. Traditionally, this technique is used in medical diagnostics, hydrophones and sonars. For the DADU submersible, miniature sonars based on PZT transducers have been developed.[11] Similarly to these applications, an MIT employs bulk acoustic waves (BAW), where the entire volume of the material is deformed. The largest displacement amplitude of the transducer is obtained at the series resonance frequency, which for a plate-type geometry is proportional to the wave velocity and indirectly proportional to the thickness of the material.

Acoustic radiation forces can be employed in a microfluidic channel to trap particles and cells suspended in water.[12–15] Generally, a standing wave field is used, and particles are trapped at pressure node positions in the channel. The direction of the acoustic radiation force is such that a stiff and high-density particle will go to a pressure node of the standing wave. In contrast, a flexible and low-density particle will be pulled into a pressure anti-node.

Acoustic manipulation by radiation force in a standing wave is considered to be long-range, in the sense that particles anywhere in the channel above an MIT are collected to a node. The standing wave is most commonly created by reflection at a surface of different acoustic impedance than the medium through which the wave is traveling from. The acoustic radiation force decreases with decreasing driving frequency and decreasing size of the object being trapped.[16] In most BAW transducer systems, the particles trapped have a diameter larger than 1 μm. Biological cells usually have a lower acoustic contrast factor (ACF) than the polystyrene beads of the same size, often used for characterizations and tests, and the efficiency of the trap needs to be high enough to meet this requirement.

Putting the MIT inside the channel is advantageous since the acoustic field in the channel does not depend on the resonance of the entire channel structure, as is the case for the most commonly used acoustic manipulation devices.[17] Hence, the mechanical attachment to the submersible body is not limited, nor is it expected that the trap will lose much energy to the surroundings upon submersion.

In a flow, an acoustically trapped particle will remain trapped as long as the radiation force exceeds the drag force. As more and more particles become trapped in a standing wave's pressure minima, the particles scatter the incident wave, which gives rise to secondary, short-range acoustic forces. These forces, in turn, act to attract the particles, gathering them into a cluster.[18]

The acoustic radiation forces are generally considered to be gentle for cells at the voltage levels employed for trapping, and a trapped particle will experience little mechanical stress. Several studies on the effects of ultrasound on the viability of cells have shown no detrimental effects. For example, earlier versions of the MIT platform were used for viability studies of yeast cell growth during 6 hours of trapping and neural rat stem cells by Acridine Orange after 15 minutes of trapping.[9]

Design

The design of the previously published MITs[9] and paraffin valves[10] was adopted to meet the requirements for the submersible, such as a compact size and high sample concentrations. The integration was performed to use the advantageous properties of the individual technologies and devices without them interfering negatively. The acoustic nodes trap particles within the microfluidic channel, and the high-pressure, latchable paraffin valves at each end ensure the pristinity of the samples.

The sampler consists of a multilayer stack of stainless steel, polyimide and glass sheets, Fig. 2. Steel sheets form the structure of the microfluidic channel and the rigid parts of the valves, whereas a polyimide sheet, (6) in Fig. 2, provides a membrane for the valves. A flexible printed circuit board (FPC), (8) in Fig. 2, provides heaters for the thermally actuated valves and circuit leads for the MITs. The MITs are integrated into holes in one of the metal sheets, (4) in Fig. 2, forming the microfluidic channel floor, while a glass sheet, (2) in Fig. 2, makes up the channel ceiling. In addition to acting as an acoustic reflector, the glass sheet also allows for visual inspection of trapped particles.

To fit into one of the instrument bays in the hull of the submersible, the sampling device is restricted to a lateral size of about 30 by 15 mm, and a couple of millimetres in height.

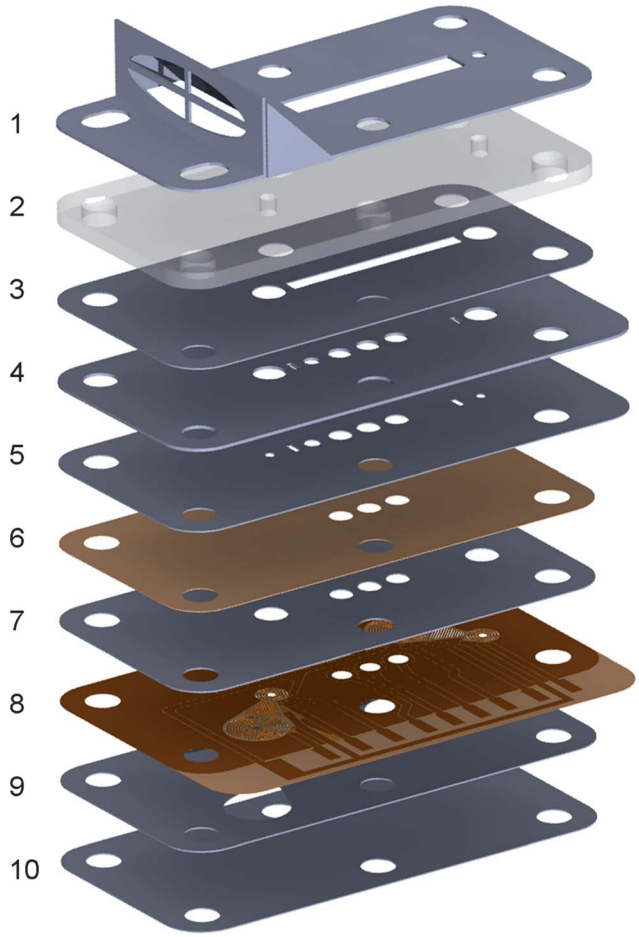

Fig. 2 Exploded view of the stack of sheets forming the sampling device: (1) cover plate with inlet funnel, (2) glass sheet, (3) flow channel sheet, (4) transducer holder sheet, (5) valve seat sheet, (6) polyimide membrane sheet, (7) paraffin top cavity sheet, (8) FPC, (9) paraffin bottom cavity sheet, and (10) back plate.

Whereas most sheets are 30 mm long and 15 mm wide, three, (4), (5) and (8) in Fig. 2, have contact pad extensions of an extra couple of millimetres to one of the sides, for easier connections during testing.

To enable a flow through the microfluidic channel, without complicating the design by including any pumps, a funnel structure, (1) in Fig. 2, raised above the surface of the device, and the rest of the submersible's hull, is used to direct water into the microfluidic channel, Fig. 1.

The sheets are either glued together, where the glue is dispensed using capillary forces, or bonded, using deposited parylene layers. The parylene is a biocompatible material,[19] acts as an electrical insulator, and offers a moisture diffusion barrier.

Along the channel floor, the three MITs, 1.0 × 1.0 mm and 200 μm thick, are suspended in holes in the transducer holder sheet using Viton. Viton was chosen as a mounting material because it is stable in the parylene bonding step, and to give the transducer a flexible mechanical boundary. Less mechanical strain at the transducer–mounting material interface is desirable to ensure good electrical contact across the evaporated conductor layer for stable, long-term operation. Three MITs provide for larger total trapping area and a degree of redundancy, in case one or two of the traps would malfunction, the device can still trap microorganisms. Together with the flow channel sheet and the glass sheet on top, a 12 mm long, 1.2 mm wide, and 110 μm deep microfluidic channel is formed, including a 10 μm thick parylene layer. At 11 MHz, 110 μm corresponds to approximately two times a half wavelength, which is twice larger than the more commonly employed half-wavelength channel height design.[13,20] As a result, two nodes or more, rather than one, are expected in the height direction for the case where the high-impedance boundary conditions of the transducer and the glass reflector dominate the behavior, Fig. 3. For instance, a triple-node design has been employed in glass capillary channels.[21]

The channel height here was governed by the available thicknesses of stainless steel sheets and the thicknesses of the deposited layer of parylene.

In order to form the acoustic standing waves, the appropriate thicknesses of the transducer, microfluidic channel and the reflective glass sheet were calculated using acoustic design principles,[9] Fig. 3. When the transducer is activated, the transducer surface displacement excites a pressure wave in the liquid and an acoustic standing wave is created between the transducer surfaces and the channel's glass ceiling, trapping the particles into clusters in the pressure nodes, Fig. 3.

To investigate the relationship between the flow speeds outside the device, relating to the estimated speed of 10–15 cm s^{-1} of the submersible, and the average flow speed through the microfluidic channel, a finite element analysis (FEA) software, COMSOL Multiphysics (ver. 4.1, COMSOL AB, Stockholm, Sweden), was utilized. A 2-D cut-through model of the device with the microfluidic channel, including the inlet funnel, was used and the volume flow rate was calculated from the simulation results. From this, the channel dimensions could be deduced.

At both ends of the trapping region in the microchannel, a paraffin valve is placed. Paraffin is a suitable actuator material for the high-pressure valves since it has a thermohydraulic volume expansion of 10–20% and a low compressibility when melted. The paraffin is here contained in cavities in the device, with sidewalls made up by the two paraffin cavity sheets, whereas the polyimide membrane sheet and the back plate sheet make up the top and bottom, respectively.[22] Sandwiched between the two paraffin cavity sheets is the FPC sheet, placing the resistive heaters within the paraffin cavity and in full contact with the paraffin volume. Each valve consists of an asymmetrically

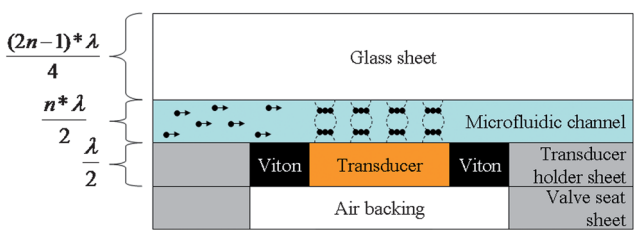

Fig. 3 Side-view schematic of the acoustic trap, showing particles flowing through the microfluidic channel. At the bottom, a Viton-suspended transducer creates acoustic standing waves between its surface and the glass sheet, trapping particles in the pressure nodes of the acoustic field.

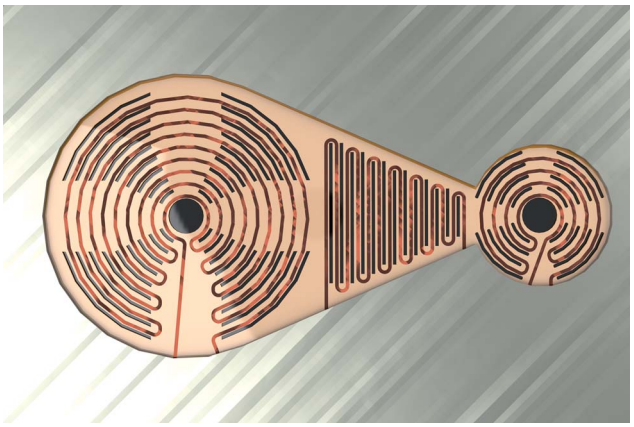

Fig. 4 CAD drawing of the paraffin cavity seen from above, with its three integrated FPC heater elements, from left to right: reservoir heater (large circular geometry), channel heater (triangular geometry) and membrane heater (small circular geometry).

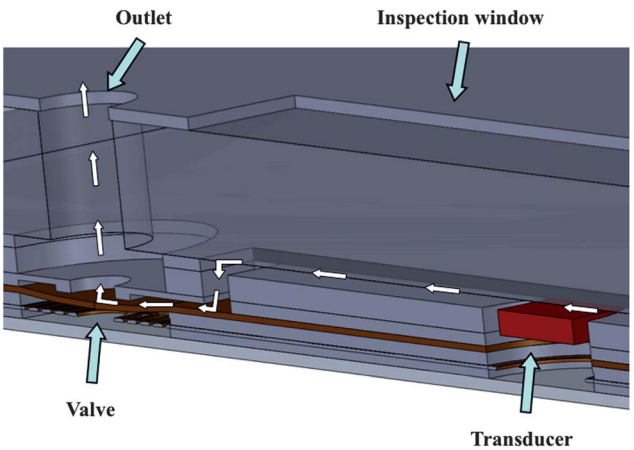

Fig. 5 Cross-sectional view of part of the assembled device, small white arrows show the fluid flow over the third transducer in the channel and the valve at the outlet. The stacked sheets Fig. 2, can be seen and the elongated inspection window at the top.

shaped paraffin cavity with three heater segments, which enables high-pressure latchable sealing, Fig. 4.

Due to the low thermal conductivity and the large amount of latent heat required for melting, a latchable operation of the valve, where the segments are activated in certain sequences, is possible by controlling the direction of the expansion and contraction associated with the solid-to-liquid phase shift of paraffin. Through this sequencing, it is also possible to refresh the current latch position without deactivating it, *i.e.* refreshing the seal of a closed valve without having to break the seal in the actuation of the valve. When activated, the expanded paraffin will deflect the membrane part of the polyimide sheet and press this against the valve seat in the sheet above, closing off the path of the flow from the microfluidic channel, Fig. 5. The valve will hold this position until the heaters are reactivated in a different sequence, enabling the paraffin to retract and lower the membrane, and thus open the channel.

Manufacturing

The steel sheets were photochemically machined (HP Etch AB, Sweden) and the polyimide sheets (Novoclad G2300, Northfield, MN, USA) were structured using standard lithography and subsequent copper wet etching ($Na_2(SO_4)_2$: H_2O, 20 g : 100 ml at 50 °C) followed by reactive ion etching (50 sccm O_2, 5 sccm Freon-23 at 100 W and 70 mtorr) of the polyimide.

The MITs were manufactured from dicing a 0.2 mm thick commercial single layer PZT plate with silver electrodes (Pz26, Ferroperm Piezoceramics A/S, Kvistgaard, Denmark) into 1 mm quadratic elements.

The transducer holder sheet, (4) in Fig. 2, was placed upside-down on a flat piece of oxidized PDMS (Elastosil RT 601, Wacker, Munich, Germany) and a diced transducer was placed in each of the three holes of the sheet. These were then glued using Viton (Pelseal Technologies LLC, Newtown, PA, USA). After the Viton had cured at room temperature, the PDMS was carefully removed and the Viton was cured for an additional hour at 180 °C to increase its mechanical strength. Excess Viton was carefully removed using a scalpel. A 100 nm thin film of gold, with a 20 nm thick adhesion layer of chromium, was evaporated onto the top surface of the sheet (Edwards III Auto 306 FL400, Edwards Ltd, UK), covering also the Viton and transducers' top surfaces, forming the ground connection for the three MITs. The evaporation step was repeated for the bottom side, this time with a shadow mask to apply the electrode layer only on the transducers' signal sides. The three MITs were then masked on the bottom side for the subsequent parylene coating step, where all sheets were coated with a 10 μm thick Parylene C layer (Plasma Parylene Systems GmbH, Rosenheim, Germany).

The middle sheets, (3)–(9) in Fig. 2, were mounted in a clamping device and aligned using guide structures. The assembly was baked in a vacuum oven, at 9 kPa and 200 °C, for 30 minutes for initial parylene bonding and to expel any air trapped between the sheets. The device was then transferred to an oven at 240 °C for 30 minutes for the final parylene bonding.

After bonding, the MITs' signal electrodes were connected to their contact pads on the FPC sheet, (8) in Fig. 2, using a column of conducting epoxy (EPO-TEK H20S, Epoxy Technology, Inc., MA, USA) and cured at 80 °C for 90 minutes. The connected MITs' resonance responses were verified using an impedance analyzer (Agilent 4395A, Agilent Technologies Inc., Santa Clara, CA, USA).

The parylene was removed from the flow channel sheet, (3) in Fig. 2, using a scalpel and fine abrasive paper for the subsequent capillary gluing of the glass sheet, (2) Fig. 2, which did not allow for the high temperature and pressure of parylene bonding. The glass sheet was diced, using a semiconductor dicing equipment (Disco DAD 361, DISCO Corporation, Tokyo, Japan) and a diamond blade, from a 4-inch 665 μm thick Pyrex wafer, which had been thinned to a thickness of 609 μm using wet etching (HF (50%) : HCl (37%) : H_2O, 5 : 1 : 5 at room temperature). Holes, 1 mm in diameter, for the inlet and outlet were drilled through the glass sheet before it was clamped against the flow channel sheet. Epoxy (EPO-TEK 301, Epoxy Technology, Inc., MA, USA) was applied and drawn in between these two sheets using capillary force. The glue was cured in an oven at 65 °C for 60 minutes.

To fill the valves with the actuator material, the device was placed up-side-down on a hot plate, at 70 °C. Small flakes of paraffin (CAS 8002-74-2, Sigma-Aldrich Co. LLC, St Louis, MO, USA) with a melting point of 48 °C were placed and melted in the cavities of the paraffin bottom cavity sheet, (9) in Fig. 2, until these were slightly overfilled in the liquid state, whereafter the device was transferred to a vacuum chamber, to expel any air trapped in the still liquid paraffin. Once solid, the excess paraffin was scraped off using a razor blade, and the parylene using a scalpel and fine graded abrasive paper.

A diced glass sheet was glued over the paraffin bottom cavity sheet, using the same capillary gluing method, but this time the glue was cured at room temperature.

Signal wires were soldered to the contact pads of the FPC sheet, and a ground wire was glued to the transducer holder sheet contact pad, using conductive epoxy (CW2400, CircuitWorks, ITW Chemtronics, Kennesaw, GA, USA).

Finally, the cover plate with a raised intake forming the water-collecting funnel, and the back plate sheet were glued to the top and bottom of the stack, respectively, using the above-mentioned capillary gluing technique.

In total, the thickness of the stacked sheets measures less than 2 mm, excluding the funnel, which extends 5 mm above the surface.

Until a sample is to be acquired, the device, mounted for instance on the DADU vehicle's hull, will be sealed, *i.e.*, have its valves latched closed, and a sterilized and neutral liquid kept within the microfluidic channel. When a sample is desired, the valves will open and water will flow from the funnel into the microfluidic channel. However, for the evaluation of the acoustic trapping capabilities and the performance of the high-pressure valves, the cover plate sheet with the raised funnel intake was omitted and microfluidic tubing attached.

One device containing the latchable paraffin valves, Device I, was manufactured for the high-pressure valve tests, and another one, Device II, containing the MITs for the initial acoustic trapping tests. A third one, Device III, was manufactured to test these operations together. For this device, the back plate sheet was exchanged for a glass sheet to enable visual monitoring of the paraffin actuators. To test the inlet funnel, a fourth device, Device IV was manufactured, containing the cover plate with the inlet funnel.

Evaluation

Valve

During the high-pressure tests, Device I was clamped in a custom-made aluminium fixture. Poly(etheretherketone) (PEEK) tubing, 1/16 inch, was mounted with ferrules (IDEX Health & Science, Oak Harbor, WA, USA) in the aluminium fixture to secure a tight seal against the inlet and outlet fluidic ports of the device. Deionized water was pumped (P-3500, Pharmacia Biotech, Uppsala, Sweden) through a pressure sensor (PA-11, Keller AG, Winterthur, Switzerland), monitoring the pressure in the system using in-house written LabView software (LabView, National Instruments Corporation, Austin, TX, USA). The pressure sensor was connected to the sampler input port, and a flow sensor (SLG1430-480, Sensirium AG, Staefa, Switzerland) to its output port where a software (Sensiview v2.2, Sensirium AG, Staefa, Switzerland) was used to monitor the flow through the system.

On closing the valves, using power supplies (QL 355P and QL 355TP, Thurlby Thandar Instruments Ltd., Huntingdon, England) connected to the resistive heaters on the FPC, the pressure in the fluidic system on the inlet valve increased as the pump continued pumping. The valve was latched using the same activation sequence as in a previous work,[10] by using the three connected actuator cavities, Fig. 4, denoted reservoir, channel and membrane, each addressed separately by using individually activated heaters. Power input was 2.4 W for 4 s, 1.0 W for 3 s, and 0.6 W for 2 s, to the heaters in the respective cavities.

The pressure was first kept above 1.1 MPa and then above 2.1 MPa for the long-term tests, until the test was aborted by manually opening the valves or until the flow sensor indicated leakage. Due to some leakage in the test setup, there was a slight continuous pressure drop in the system throughout the tests, and thus the pump had to be reactivated at regular intervals to restore the pressure, and keep it above the set limit. A leakage through the valve was detected both as an increase in the overall system pressure drop rate and as flow by the flow sensor.

A breach test was also performed, where the pump ramped the pressure up from atmospheric pressure (100 kPa) to over 20 MPa in 13 minutes, and then held there until any leakage through the valve occurred, as indicated by a sudden drop in pressure and a registered flow rate.

Channel flow

Device IV was used for flow rate evaluation of the microfluidic channel. The microfluidic channel was filled with ink-dyed water using a syringe. The device was mounted on a flat cantilever beam and held horizontally at the long side inside a water tank. Using an aquarium pump (Eheim GmbH & Co. KG, Deizisau, Germany) mounted in one of the corners and directed along the opposite side, the tank water was set in motion. The flow speed around the device created by the test setup was estimated to be 10–15 cm s^{-1} by observing suspended particles, and the flow in the microfluidic channel by observing the recession of the dyed water as clean water was forced in through the intake.

Trapping

For initial tests of the particle trap, and later for a complete system test, Device II and III were used, respectively. Polyethylene tubes (Clay Adams 427406, Becton Dickinson Intramedic, MD, USA) were glued using an epoxy (Bostic Epoxy Rapid, Total S.A., Paris, France) to the inlet and outlet holes in the glass sheet. The device was mounted upside down in a live cell inverted microscope (Eclipse TE2000-U, Nikon Corporation, Tokyo, Japan) using a custom-built holder. The inlet tube was connected to a syringe containing deionized water with suspended 1.9 μm diameter green fluorescent polymer microspheres (Duke Scientific Corporation, CA, USA). Polysorbate 20 (Tween 20, Alfa Aesar GmbH, Germany) was added to the solution to disperse the diluted particles. The fluorescent particles were used for characterization of the sampler's trapping abilities, since they exhibit a strong fluorescence, making them easy to track and count. The concentration, verified using a Bürker cell chamber, was 8×10^5

particles per ml, which is within the range of the concentration of microorganisms in marine and fresh water environments,[23] and approximately the concentration of microorganisms of similar size that were found in a lake beneath Vatnajökull ice cap.[7]

The fluid was flushed into the microfluidic channel where the MITs were activated using a sinusoidal signal of 12.4 V_{pp} at a measured series resonance frequency of 11 MHz (Agilent 33120A, Agilent Technologies, Santa Clara, CA, USA).

To analyze the results, two cameras attached to the microscope were used: a cooled CCD camera (RTKE SPOT, Diagnostic Instruments Inc., Sterling Heights, MI, USA) using an accompanying computer software (SPOT v.4.0.9, Diagnostic Instruments Inc., Sterling Heights, MI, USA), and a CoolPix 4500 digital camera.

To investigate the strength of the acoustic trap, particles were trapped at a flow rate of 0.5 μl min^{-1} and allowed to accumulate into clusters in the nodes for about one minute before the flow rate was stepped up, in steps of 0.25 μl min^{-1}, until the entire cluster of particles broke free from the trap, or the clusters were stripped from particles, one after the other, by the flow.

The acoustic trap's ability to capture particles was also investigated by activating an MIT at flow rates of 2, 5, 10 and 15 μl min^{-1}. After 1.5, 3 and 6 minutes for each flow rate, the MIT was deactivated and the amount of released particles quantified for each case using camera images.

Furthermore, one of the latchable valves was activated during sampling, to investigate its effect on the trapped particles.

In addition, a microorganism model particle of cultured green fluorescent protein (GFP) marked yeast cells in Dulbecco's phosphate buffered saline (PBS) solution (D8537, Sigma-Aldrich Co. LLC, St Louis, MO, USA) was tested. Glucose, to a concentration of 2%, had been added in this mixture to activate the promoter of the GFP, and make the cells fluorescent. The solution was introduced into the microfluidic channel in the same way as the fluorescent particles.

Results

With the above-described method, devices with working acoustic traps and high-pressure latchable valves have been manufactured and tested, and verified to be able to trap fluorescent polymer microspheres and yeast cells suspended in water flowing through the system.

Valve

For the pressure test of the valves, using Device I, the fluidic system was subjected to a pressure of at least 1.1 MPa for 25 hours during which a stable pressure and no flow, *i.e.* no leakages, had been registered. However, when reviewing the recorded pressure and flow rate data, a leakage of approximately 50 nl min^{-1} was discovered after a time of 17 hours. This leakage lasted for 1.5 hours before the pressure, which then had reached 1.5 MPa, stabilized and the flow rate associated with the leakage stopped. After this, the system remained stable for the rest of the time.

A second long pressure test was performed, this time above 2.1 MPa. After 19 hours, a leakage of approximately 50 nl min^{-1} was detected. This time the leakage was remedied by reactivating the valve with the closing sequence.

In the breach test, no leakage was observed until a pressure of 12.5 MPa was reached. Above this pressure, a small increasing leakage was registered before a catastrophic drop in pressure and a rapid increase in flow rate were registered after a total time of 13 minutes. The pressure had then reached 20.2 MPa, and been at that level for 2 minutes before the valve seal finally failed completely.

The energy consumptions for the closing and opening of a valve during these tests were measured to be 13.8 and 8.4 J, respectively.

Channel flow

In FEA simulations and calculations, the dependence between the external flows of the device and the internal flow, through the microfluidic channel was investigated, Table 1.

For Device IV, with the raised funnel mounted on it, Fig. 6, an estimated average flow rate of 10–15 cm s^{-1} around the device resulted in a flow rate in the microfluidic channel of approximately 0.7 mm s^{-1}, corresponding to 5.5 μl min^{-1}.

Table 1 FEA results of the flow rate in the microfluidic channel *versus* external flow rate

External flow/cm s^{-1}	Internal flow/μl min^{-1}	Internal flow/mm s^{-1}
6.6	2.0	0.3
10.6	5.0	0.6
15.1	10.0	1.3
18.5	15.0	1.9

Fig. 6 Photograph of device IV, 30 mm long and 15 mm wide, with a raised intake funnel, 5 mm high. The intake has a coarse grid to prohibit larger particles from entering and clogging up the intake. Behind the intake, an elongated opening in the cover sheet enables viewing of the microfluidic channel beneath. At the end of this window is the outlet of the microfluidic channel.

Trapping

For the initial particle trapping test using Device II, as the fluid with the water-suspended fluorescent particles flowed over an MIT surface, left in Fig. 7, the MIT was activated and within a few seconds the particles were captured into clusters in the nodes of the standing wave field, right in Fig. 7.

For further investigations, Device III was used. Particles were trapped in the middle of the channel up to a flow rate of 0.5 μl min^{-1}. Above this, the particles were travelling too fast for the

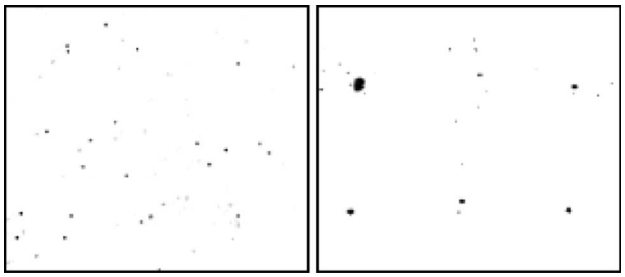

Fig. 7 Microscopic view through the glass sheet into the microfluidic channel above one of the MITs in Device II. The free water-suspended 1.9 μm diameter polystyrene particles (left) accumulate at the acoustic pressure nodes as the MIT is activated (right). The vertical trapping position in the channel is here away from the transducer and reflector surfaces. The B/W image has been inverted for better visualization of the particles. The field of view covers a quarter of the MIT.

acoustic standing wave to trap them. Even if no significant trapping could be observed above this flow rate, the clusters of particles captured at a lower flow were found to withstand a flow rate of about 1.5 μl min^{-1} before being dragged away from the middle nodes. However, the surfaces of the transducer, Fig. 8, and glass surfaces were found to trap and hold particles for all the flow rates tested, Fig. 9. At the particle concentrations and collection times evaluated, the trap was not saturated.

When one of the valves was closed during sampling, the captured clusters of particles were dislodged from the acoustic traps. However, the particles were observed to still be within the length of the microfluidic channel.

When introducing the GFP-marked yeast cells into the microfluidic channel, these were successfully captured and held in the acoustic trap just as well as the particles.

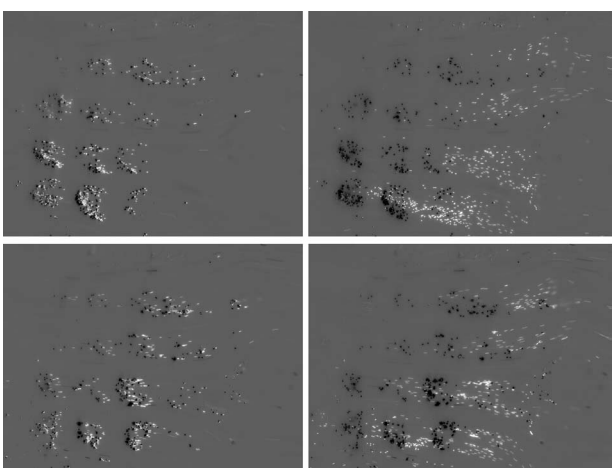

Fig. 8 Sequential images of the 1.9 μm diameter polystyrene particles captured on an MIT's surface in Device III after 6 minutes activation at a flow rate of 10 μl min^{-1} (top half) and 15 μl min^{-1} (bottom half). The left images are taken just as the particles have been released, and the right images a couple of seconds later, when the particles have spread out in the flow. White dots represent the particles' locations after the release, and black dots where the trap held them. The flow of the water is from left to right. The field of view, 1.2 by 1.6 mm, encompasses the surface of one MIT.

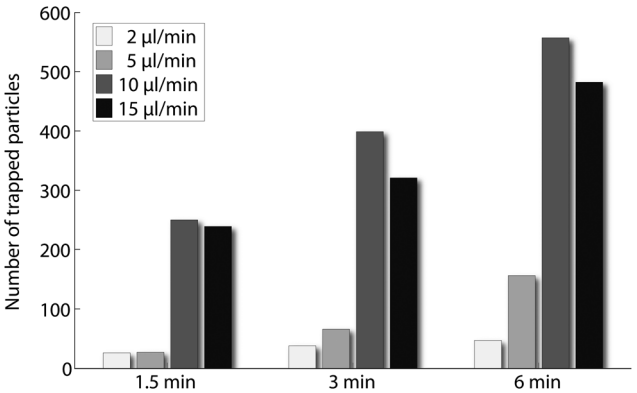

Fig. 9 Recorded number of trapped particles on the MIT surface, Fig. 8, plotted against time at different flow rates.

The power consumption for the MIT during trapping was measured to be 78 mW. For the different trapping times, this results in an energy consumption of 7.0 J, 14.0 J, and 28.1 J for the respective sampling times.

Discussion

Two devices were initially used to test the valves and the trapping capabilities separately. These two features were then incorporated into a third device, where the trapping of particles and the latching of the valves were demonstrated together. Due to the use of a glass sheet to visualize valve actuation in the third device, this device could not perform high-pressure tests. However, it is the authors' firm belief that the performance and functionality of the different devices are straight-forward to combine in a single device.

Throughout the design and manufacturing, the transducers have been continuously monitored during the different steps to verify their function and performance. These are influenced by several parameters including, for instance, the transducer material's electromechanical coupling and losses in the material, the electrical matching to the drive electronics, the thicknesses of the fluidic cavity, glass reflector layer and transducer and the transducer mounting boundary conditions.

The pressure tests of the valves showed that these worked as intended. The pressure was held above 2.1 MPa for 19 hours before a leakage of 50 nl min^{-1} occurred. This small leakage corresponds to a valve opening of only 400 nm, which coincides with the size of the smallest known living organism, the *Nanoarchaeum equitans* microorganism.[24] In addition to being small, the leakage was found to be remedied by re-activating the valve. Thus, the valve could be used for longer time frames by periodically reactivating the valve, refreshing its seal. With an energy consumption of 13.8 J every 19 hours, this results in an average power consumption of 0.20 mW for each valve. Using an ordinary mobile phone battery of 1300 mA h, which is equivalent to 17 kJ, this would keep the microfluidic channel sealed for well over a year.

The valve could be used at higher pressures, reaching 12.5 MPa in the short-time pressure test, before a small leakage occurred. As the pressure continued to increase, the leakage registered through the valve increased until the valve seal burst

above 20 MPa. The short-time performances of the valve match the design goal of the DADU submersible, to be able to operate at a depth of 1000 metres, corresponding to a pressure of 10 MPa.

The acoustic trapping was demonstrated for 1.9 μm polystyrene beads and yeast cells. The acoustic traps were able to trap the polystyrene particles in the middle of the microfluidic channel, but also close to the transducer and glass surfaces. Three nodes were thus observed, rather than two, Fig. 3, and further investigations are needed to fully explain the position of the multiple nodes in the trap. Irregularities in the manufacturing process such as the position of the MITs, and the thickness of the parylene layer can generate variations of the channel height. Furthermore, variations in the glass layer thickness will influence the multilayer design. If the boundary condition of the outer glass layer can be considered to be clamped to some degree by the outer steel layer this will also affect the multilayer design. These factors may enable operation with three nodes rather than two nodes. In the case of glass capillary devices, the use of twice the channel height enabled operation at the third harmonic.[21] Generally, more advanced analysis of the system performance can be performed based on channel eigenmodes,[17] total resonance structure eigenmodes,[17] multilayered acoustic resonance structures[20] and the acoustic near field.[25] However, the ability to trap particles near the MIT and glass surfaces is advantageous for the application. For higher flow rates, where the acoustic nodes in the center of the channel could neither trap, nor hold on to particles trapped at weaker flows, the lower flow velocities closer to the bottom and the top of the channel in a parabolic flow profile still enabled trapping in those nodes.

A majority of the trapped particles was trapped at the MIT's surface, with a maximum number at a flow rate of 10 μl min^{-1}, Fig. 9. The smaller numbers of trapped particles at lower flow rates are believed to be related to the smaller number of particles being brought to the trapping nodes. At 15 μl min^{-1}, even though the higher flow rate brings in more particles, it was observed that more particles were also torn away from the nodes by the flow. It was also observed that the areas in which the particles were trapped over the transducer surface were shifted downstream at higher flow rates, Fig. 8. This is interpreted as a result of the higher flow rate, being able to transport the particles further downstream, *i.e.* to the right in the images, before they are forced down and trapped against the MIT's surface by the acoustic force.

Since the acoustic wavelength in water is dependent on the speed of sound, which in turn increases with the pressure, temperature and salinity, variation of these factors is expected to affect the trapping efficiency. To roughly determine how large these effects are, the induced change in operating frequency for a full-wavelength standing wave cavity was investigated using known sound speed dependences on pressure, salinity and temperature.[26] It was found that in the temperature range of 0 to 35 °C, the frequency shift is 0.87 MHz, in the salinity range of 0 to 45 ppt, the frequency shift is 0.50 MHz, and in the depth range of 0 to 1000 m, the frequency shift is 0.15 MHz. It should be noted that temperature generally decreases with depth while pressure and salinity increase. The profile of sound speed with depth decreases to a minimum at a depth of several hundred metres, then increases again with increasing depth.[26]

The MITs are rather broadbanded, with a FWHM of 0.8 MHz as obtained from the real part of admittance. During testing, the sampler was found to be able to trap particles in a frequency range of 9 to 11.5 MHz, at room temperature (atmospheric pressure and using deionized water). It is therefore estimated that the acoustic traps would be able to function during conditions with the above variations of pressure, temperature and salinity. An approach is to have interchangeable devices set for narrow-range specific collection parameters, where the center channel resonance frequencies are optimized for a specific target depth, temperature and salinity.

A similar acoustic trap has been demonstrated for trapping polystyrene particles between 1.8 and 10 μm in diameter.[9] According to the authors' knowledge the exact ACF of microorganisms of interest is yet to be determined. The ACF of a range of cell types relative to a polystyrene bead has recently been measured and calculated to be in the range of 0.3–0.7.[27,28] Values as low as 0.06–0.23, relative to polystyrene particles, have been obtained for some cell types.[29,30] The ACF value also varies within cell populations.[27,29,30] Assuming microorganisms with ACF in the range of 0.5, and where the acoustic radiation force is proportional to the ACF and the size of the cells, it is expected that the type of devices evaluated here enables trapping of microorganism in the approximate range of 2.5–10 μm. By using a single crystalline piezoelectric material with high electromechanical coupling factor, operated at a voltage of 18 V_{pp} and with the same principal design, the trapping of 0.4 μm diameter polystyrene particles has been demonstrated.[31] Potentially, changing the piezoelectric material may enable trapping also of microorganisms with submicrometre diameters, especially if the particle concentrations are high enough for secondary acoustic forces to also contribute or if seeding particles are used.[32]

Due to mechanical and dielectric losses in the PZT material, heating associated with the MIT's operation can couple to the microfluidic channel. A quadratic relationship between the driving voltage and the temperature has been shown, where a temperature increase of a couple of degrees centigrade occurred.[9] By decreasing the voltage, this increase in temperature should be less.

Using the same energy consumption example as for the valves, an ordinary mobile phone battery should be able to keep an MIT, consuming 78 mW, active and sampling for over 2.5 days.

As a valve is closing, water above its membrane will be displaced. In the event that one of the valves shuts before the other, the actuation will displace water through the channel and possibly dislodge the sample held in the acoustic trap, risking to expel the sample completely from the microfluidic channel, if it is not correctly dimensioned. In this design, one actuated valve could create a displacement of the samples 0.5 mm away from the valve. In fact, the expansion of all the paraffin would in a worst-case scenario give rise to a displacement of 1.7 mm. However, the smallest distance between a transducer and one of the valves is 2.8 mm, so not even the expansion of all paraffin presents any risk of expelling the sample. During trapping tests, only one of the valves was actuated, creating a mass displacement flow in the microfluidic channel. By this, trapped particles were found to dislodge from the acoustic trapping nodes. However, the particles were still well within the microfluidic channel.

When activating the different heater components of the valve in the latching sequence, it was observed that they affected the flow in the microfluidic channel differently. As the paraffin around the membrane heater was melted, the flow and the particles in the acoustic traps were pushed away from the valve as was expected. However, as the paraffin around the reservoir and channel heaters was melted, the flow reversed its direction and went towards the valve. As these paraffin cavities are situated to the side of the microfluidic channel, and since this test was performed when the device was not clamped, it is believed that this phenomenon arose due to the buckling of the device by the expanding paraffin. However, no trapped particles were observed to be lost from the microfluidic channel due to this.

The raised inlet funnel was able to force water, flowing around the sampler at a rate comparable to the speed the DADU submersible would have through the water, into the microfluidic channel, at a rate suitable for trapping the particles. The FEA simulations show that the flow rate through the microfluidic channel has a quadratic dependence on the flow around the device, at least in the flow range of the simulation, Table 1. For a different funnel opening size, grid pattern and funnel angle, the relationship between inner and outer flow rates would be different. The funnel geometry can be designed to match the desired range of flow velocities in the channel. However, dependence on an external flow to operate is not optimal for certain applications, for instance when sampling at very precise locations is needed. In addition, the raised inlet funnel presents a risk of a larger object clogging it. A modification could be to include a peristaltic pump[33] in the microfluidic channel. The flow through the sampler could then be better controlled, without the need of an inlet funnel. Additionally, the use of an extended sampling nozzle could enable more defined and specific sampling areas.

To mitigate the risk of valve leakage and contamination of the collected sample, an expandable diaphragm could be included in the microfluidic channel, to compensate for the external pressure changes, and thus relieve the valves from handling extreme pressure differences.

In underwater applications where operation in environments warmer than the 48 °C melting point of the paraffin used, such as taking samples from the rich microbial life found at hydrothermal vents,[6,34] there exists paraffin with melting points up to 150 °C,[35] which could possibly be substituted for.

To remotely detect the trapping progress in the microfluidic channel, the sample's effect on the ultrasonic parameters could possibly be used as a measure of captured quantity.[36]

The device itself could be adjusted to suit various other lab-on-a-chip applications. For instance, by changing the voltage, and consequently the acoustic radiation force, particles of different types could be discriminated.[37] Another possibility could be to use the device as a cultivating chamber, instead of flushing out the microfluidic channel upon returning from a mission. Nutrient broth could be provided through the inlet, encouraging the trapped microorganisms multiplication in the nodes, while waste products are flushed through the outlet, as has been done with yeast cells in a similar acoustic trap.[9] Therefore, the sampler presented here has a number of potential applications in addition to collecting samples onboard the miniaturized submersible explorer.

Conclusions

The high pressure, latchable valves could hold a pressure above 2.1 MPa for 19 hours, and longer when re-activating the valve, and up to 12.5 MPa for short times without leakage.

The acoustic trap was able to trap particles in flow rates up to 15 μl min^{-1}, corresponding to an 18.5 cm s^{-1} external flow rate.

The acoustic trap has also successfully captured water-suspended yeast cells and together with the high-pressure valves, shows good potential to be able to enrich and store samples taken from previously unreachable underwater environments.

Acknowledgements

The authors would like to acknowledge Maryam Montazerolghaem and Zhigang Wu at the Department of Engineering Sciences, Uppsala University for their support and helpful discussions with the fluorescent samples and Johan Sundqvist, also at the Department of Engineering Sciences, for discussions and support relating to electronic measurements. The authors would also like to thank Mojzita Dominik at the Technical Research Centre of Finland, for providing the GFP-yeast cells. Parts of this work were supported by MISTRA—the foundation for strategic environmental research, Sweden, and the Swedish Research Council.

Notes and references

1 D. M. Karl, *Nat. Rev. Microbiol.*, 2007, **5**, 759–769.
2 J. Lunine, *Astrobiology: A Multidisciplinary Approach*, Benjamin-Cummings Pub Co, 2004.
3 S. J. Niskin, *Deep-Sea Res. Oceanogr. Abstr.*, 1962, **9**, 501–502.
4 L. E. Bird, A. Sherman and J. Ryan, *Oceans Conference*, Vancouver, BC, 2007.
5 J. G. Bellingham, B. Hobson, M. A. Godin, B. Kieft, J. Erikson, R. McEwen, C. Kecy, Y. Zhang, T. Hoover and E. Mellinger, *2010 Ocean Sciences Meeting*, Portland, OR, 2010.
6 A. Behar, J. Matthews, K. Venkateswaran, J. Bruckner and J. Jonsson, *Cah. Biol. Mar.*, 2006, **47**(4), 443–447.
7 E. Gaidos, V. Marteinsson, T. Thorsteinsson, T. Jóhannesson, Á. Rúnarsson, A. Stefansson, B. Glazer, B. Lanoil, M. Skidmore, S. Han, M. Miller, A. Rusch and W. Foo, *ISME J.*, 2009, **3**, 486–497.
8 J. Jonsson, J. Sundqvist, H. Nguyen, H. Kratz, M. Berglund, S. Ogden, K. Palmer, K. Smedfors, S. Wagner and G. Thornell, *International Astronautical Congress*, Cape Town, South Africa, 2011.
9 M. Evander, L. Johansson, T. Lilliehorn, J. Piskur, M. Lindvall, S. Johansson, M. Almqvist, T. Laurell and J. Nilsson, *Anal. Chem.*, 2007, **79**(7), 2984–2991.
10 S. Ogden, R. Bodén and K. Hjort, *J. Microelectromech. Syst.*, 2010, **19**, 396–401.
11 J. Jonsson, E. Edqvist, H. Kratz, M. Almqvist and G. Thornell, *IEEE Trans. Ultrason. Ferroelectr. Freq. Control*, 2010, **57**, 490–495.
12 L. A. Kuznetsova and W. T. Coakley, *Biosens. Bioelectron.*, 2007, **22**(8), 1567–1577.
13 J. Nilsson, M. Evander, B. Hammarström and T. Laurell, *Anal. Chim. Acta*, 2009, **649**, 141–157.
14 W. T. Coakley, *Trends Biotechnol.*, 1997, **15**, 506–511.
15 D. Bazoua, W. T. Coakleya, K. M. Meekb, M. Yangc and D. T. Phamc, *Colloids Surf., A*, 2004, **243**(1–3), 97–104.
16 L. P. Gor'kov, *Sov. Phys. Dokl.*, 1962, **6**, 773–775.
17 H. Bruus, *Lab Chip*, 2012, **12**, 20–28.
18 L. A. Kuznetsova, D. Bazou and W. T. Coakley, *Langmuir*, 2007, **23**(6), 3009–3016.
19 E. Meng, P. Y. Li and Y. C. Tai, *J. Micromech. Microeng.*, 2008, 18.
20 M. Hill, *J. Acoust. Soc. Am.*, 2003, **114**, 2654–2661.
21 B. Hammarström, M. Evander, H. Barbeau, M. Bruzelius, J. Larsson, T. Laurell and J. Nilsson, *Lab Chip*, 2010, **10**, 2251–2257.

22 S. Ogden, J. Jonsson, G. Thornell and K. Hjort, *Sens. Actuators, A*, 2011, DOI: 10.1016/j.sna.2011.11.027.
23 W. B. Whitman, D. C. Coleman and W. J. Wiebe, *Proc. Natl. Acad. Sci. U. S. A.*, 1998, **95**(12), 6578–6583.
24 H. Huber, M. J. Hohn, R. Rachel, T. Fuchs, V. C. Wimmer and K. O. Stetter, *Nature*, 2002, **417**, 63–67.
25 T. Lilliehorn, U. Simu, M. Nilsson, M. Almqvist, T. Stepinski, T. Laurell, J. Nilsson and S. Johansson, *Ultrasonics*, 2005, **43**(5), 293–303.
26 R. J. Urick, *Principles of Underwater Sound*, Peninsula Publishing, Los Altos Hills, 1983, ch. 5.
27 D. Hartono, Y. Liu, P. L. Tan, X. Y. S. Then, L.-Y. L. Yung and K.-M. Lim, *Lab Chip*, 2011, **11**, 4072–4080.
28 M. Settnes and H. Bruus, *Phys. Rev. E: Stat., Nonlinear, Soft Matter Phys.*, 2012, **85**, 016327.
29 P. Augustsson, R. Barnkob, C. Grenvall, T. Deierborg, P. Brundin, H. Bruus and T. Laurell, *μTAS Conference 2010*, Groningen, The Netherlands.
30 R. Barnkob, P. Augustsson, C. Magnusson, H. Lilja, T. Laurell and H. Bruus, *μTAS 2011*, Seattle, Washington, USA.
31 S. S. Guo, L. B. Zhao, K. Zhang, K. H. Lam, S. T. Lau, X. Z. Zhao, Y. Wang, H. L. W. Chan, Y. Chen and D. Baigl, *Appl. Phys. Lett.*, 2008, **92**(21), 213901.
32 B. Hammarström, T. Laurell and J. Nilsson, *μTAS 2011*, Seattle, Washington, USA, pp. 1707–1709.
33 S. Svensson, G. Sharma, S. Ogden, K. Hjort and L. Klintberg, *J. Microelectromech. Syst.*, 2010, **19**, 1462–1469.
34 W. Martin, J. Baross, D. Kelley and M. J. Russell, *Nat. Rev. Microbiol.*, 2008, **6**(11), 805–814.
35 M. Freund, R. Csikos, S. Keszthelyi and G. Mozes, *Paraffin products: properties, technologies, applications*, Elsevier Science Publishing Company, Amsterdam, 1982.
36 L. Elvira, F. Montero de Espinosa Freijo, P. Resa and J. R. Maestre, *Revista de Acústica*, 2002, **XXXIII**.
37 V. Norris, M. Evander, K. M. Horsman-Hall, J. Nilsson, T. Laurell and J. P. Landers, *Anal. Chem.*, 2009, **81**(15), 6089–6095.

